Global control of attosecond photoionization of atoms through XUV dispersion

Kamal P. Singh[1,2] and Jan M. Rost[2]

[1]*Department of Physical Science, Indian Institute of Science Education and Research Mohali, Sector 81, S.A.S. Nagar, Manauli 140306, India*

[2]*Max Planck Institute for the Physics of Complex Systems, Nöthnitzer Strasse 38, 01187 Dresden, Germany*

(Received 25 November 2014; published 27 January 2015)

We investigate attosecond control of photoionization of helium subject to an IR pulse and a phase-shaped XUV pulse by numerically solving the time-dependent Schrödinger equation. A series of several subcycle oscillations in photoionization at one-half, one-quarter, one-sixth, and one-eighth IR cycles is observed due to high-order multiphoton quantum path interferences between IR and XUV harmonics. A global control of net photoionization is demonstrated by controlling quantum phases of these subcycle ionization channels by introducing various linear, quadratic, and random phase dispersions in the XUV harmonics. Remarkably, for a phase randomized XUV pulse the attosecond resolution in the form of subcycle oscillations in such electronic processes is preserved and their control is significantly enhanced compared to the case of a transform-limited attosecond pulse train. These features are generic and robust over a range of IR intensities and XUV spectra.

DOI: 10.1103/PhysRevA.91.013415 PACS number(s): 32.80.Qk, 32.80.Rm, 02.50.Ey, 42.50.Hz

I. INTRODUCTION

Attosecond coherent control of electronic processes in atoms or molecules is of fundamental importance in atto-science [1–6]. One of the key tools to achieve this objective has been the combined action of an attosecond pulse train (APT) synthesized from phase-locked high harmonics which is inherently synchronized with the driving IR pulse. Due to attosecond bursts in the transform-limited APT, electron wave packets (EWPs) can be precisely launched in time-delayed IR pulses, which forms the basis for attosecond control of various phenomena such as electron localization in molecules [7], atttosecond wave-packet interferometry [8,9], control of XUV transparency in He [10], and control of photoionization [11]. In general, the attosecond electronic dynamics is hard to interpret due to complex interaction between XUV and IR pulses. It is therefore desired to establish generic properties that are globally applicable to attosecond control of electronic processes.

With a pioneering experiment Johnsson *et al.* [11] demonstrated the first attosecond control of atomic photoionization in the form of half-cycle oscillations in the He^+ yield as a function of time-delay between APT and IR pulses. Since the APT was composed of the 11th to 17th odd harmonics in their experiment, this phenomenon was interpreted as interference between attosecond EWPs created by successive attosecond pulses in the APT [11,12]. Subsequent experiments on attosecond photoionization unveiled its extreme sensitivity to the XUV spectrum due to atomic resonances [13], measured quantum phases using double IR pulses with APT [14], and generalized this idea to small molecules [15,16]. Additional theoretical studies also provided detailed insight into the mechanism of the half-cycle oscillations [12,17,18]. Recently, similar oscillations were also observed in transient absorption of XUV in He [19,20]. However, many aspects of such attosecond initiated electronic processes, e.g., using XUV pulses beyond the standard APT, are not yet fully explored.

Here we propose a global control scenario for electronic processes employing arbitrarily shaped high harmonics XUV pulses, which are generated by exploiting their phase degree of freedom (where transform-limited APT is only a rigid realization). We show a generic series of subcycle oscillations (in addition to the half-cycle one) at one-quarter, one-sixth, and one-eighth IR cycles for XUV pulses. Their spectral contrast versus IR peak intensity is also studied. Employing distinct pairs of the harmonics we isolate interference between multiphoton IR and XUV photons corresponding to each photoionization channel. Due to the superposition of these subcycle oscillations, the resulting temporal structure becomes complex even in the simple atomic system. Remarkably, when we add various phase dispersions such as linear, quadratic, and random phases in the XUV frequencies the contrast of net photoionization can be enhanced compared to the transform-limited APT. These results could open new avenues for attosecond control and for understanding electronic processes initiated by arbitrarily shaped XUV pulses.

II. DESCRIPTION OF MODEL

We consider a single active electron model of a He atom. Due to the application of both a linearly polarized laser field, $F_{\rm ir}(t)$, and a XUV field, $F_{\rm uv}(t)$, the electron dynamics is effectively confined to one-dimension (1D) along the polarization axis [21]. The simplified 1D Hamiltonian of the driven He atom is given as [atomic units (a.u.), $\hbar = m = e = 1$, are used unless stated otherwise]

$$H(x,t) = \frac{\hat{p}^2}{2} + V(x) + x\{F_{\rm ir}(t) + F_{\rm uv}(t)\}, \qquad (1)$$

where x is the position of the electron and $\hat{p} = -i\,\partial/\partial x$ is the momentum operator. The potential is approximated by a nonsingular Coulomb-like form, $V(x) = -1/\sqrt{x^2 + a^2}$. Such a soft-core potential with parameter a has been routinely employed to study many intense-field phenomena such as multiphoton or tunnel ionization and plateau in the high harmonic generation [21]. Using $a^2 = 0.483$, the ionization potential of our model was $I_p = 0.904$, which matched with the first I_P of He.

The external perturbations [the last term in Eq. (1)] are dipole-coupled to the atom. The laser field is a nonresonant

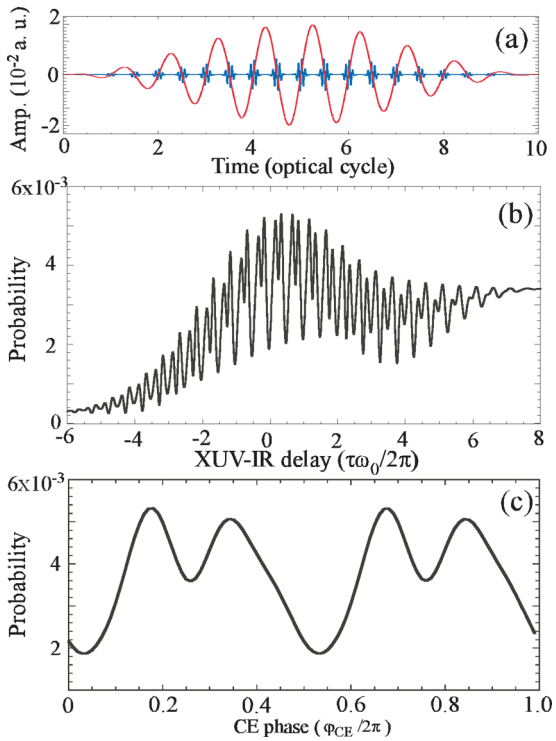

FIG. 1. (Color online) (a) An example of superimposed APT and IR pulses for zero delay. (b) Ionization probability $P(\tau)$ as a function of the time delay between APT and IR pulses. Positive (negative) delays correspond to action of the IR pulse after (before) the XUV pulse. $F_0 = 0.03$, $F_{0uv} = 0.02$, and $\varphi_{CE} = 0$. (c) The ionization probability $P(\varphi_{CE})$ versus the CE phase for $\tau = 0$.

femtosecond pulse described by

$$F_{ir}(t) = f(t)F_0 \sin(\omega_0 t + \varphi_{CE}). \quad (2)$$

Here F_0 is the peak amplitude of the pulse, ω_0 is its central angular frequency, and φ_{CE} is the carrier-to-envelope phase (CEP). *f(t)* defines a smooth $\sin^2$ envelope defining a pulse duration of $20\pi/\omega_0$. The XUV pulse $F_{uv}(t)$ is composed of $N = 6$ high-order odd harmonics of the fundamental laser field which can be written as

$$F_{uv}(t) = f'(t)\frac{F_{0uv}}{N}\sum_{n=N_i}^{n=N_f} \sin(\omega_n t + \phi_n), \quad (3)$$

where F_{0uv} is the peak amplitude of the XUV pulse, and ω_n and ϕ_n are the frequencies and spectral phases of the harmonics, respectively. The pulse envelope $f'(t)$ is chosen to be identical to that of the IR pulse.

When all the phases are locked to zero $\phi_n = 0$, we obtain a Fourier-transform-limited APT with the shortest possible attosecond bursts of around 200 as in our case. Since the XUV spectrum contains only odd harmonics these bursts repeat twice per IR cycle [Fig. 1(a)]. Note that when we introduce dispersion in the harmonics, i.e., when the phases ϕ_n are scrambled arbitrarily, the pulse shape may not contain the shortest bursts. It could even look "chaotic" due to random interference of the harmonic fields [22,23].

The atomic ionization under combined action of these two perturbations is computed by numerically solving the corresponding time-dependent Schrödinger equation,

$$i\frac{\partial\Psi(x,t)}{\partial t} = H(x,t)\,\Psi(x,t), \quad (4)$$

using the split-operator fast Fourier transform algorithm [23,24]. The initial state $|\Psi_0\rangle$ was the *ground state* of the system, obtained by imaginary time-propagation [24]. The ionization probability P of the atom was computed by integrating the ionization flux leaking into the continuum from both sides as $P = \int_0^\infty (J_R(x_+,t) + J_R(x_-,t))dt$, where the flux is defined as $J_R(x_\pm,t) = \pm\mathrm{Re}[\Psi^*\,\hat{p}\,\Psi]_{x_\pm}$, and $x_\pm$ are distant points (typically ± 500 a.u.) near the absorbing boundary. The ionization rate is integrated over a sufficiently long time interval to obtain the corresponding total ionization probability.

III. RESULTS

First, we verify that the Hamiltonian of Eq. (1) is realistic by reproducing the observed attosecond control of photoionization of He subjected to both the APT and IR pulses. The APT was synthesized from six phase-locked odd harmonics ($N_i = 9$ to $N_f = 21$ with $\phi_n = 0$) of the laser frequency. For the IR amplitude $F_0 = 0.03$ a.u. and the XUV amplitude $F_{0uv} = 0.02$ a.u., the ionization probability exhibited oscillations when APT-IR delay τ was varied as shown in Fig. 1(b). These oscillations were the strongest when APT and IR pulses overlapped (around $\tau = 0$) and gradually vanished when these pulses acted sequentially. Several experimental [11,13,14] and theoretical works [12,17,18] observed such features on photoionization of He; however, only half IR-cycle periodicity has been reported so far.

Instead of the time delay τ we vary in the following the carrier envelope phase φ_{CE} for fixed delay $\tau = 0$ to explore features of attosecond control of photoionization in the subcycle regime. This procedure is convenient due to the periodicity of the IR pulses with φ_{CE}. Figure 1(c) shows identical periodic structure in $P(\varphi_{CE})$ within one IR cycle that proves the equivalence of the CEP and time-delay τ near the zero delay region.

We investigate now the IR-assisted photoionization of helium subjected to various phase-shaped XUV pulses. They are generated by introducing various forms of dispersions such as linear, quadratic, and random in their spectral phases whereby the frequency content of the XUV pulses is not altered. Considering the simple case where we add a stationary linear phase-slip between consecutive harmonics of the form, $\phi_i = (i-1)\Delta\phi$, where $i = 1,2,\ldots$ is the counting index for the successive harmonics. For $\Delta\phi = \pi/3$, the shapes of the XUV pulse and corresponding $P(\varphi_{CE})$ are shown in Figs. 2(a) and 2(b). Interestingly, the ionization oscillations remain preserved but show a complex structure.

Similarly, when we introduce a stationary quadratic dispersion between the harmonics as, $\phi_i = i(i-1)\Delta\phi$, the XUV pulse [for $\Delta\phi = \pi/6$ Fig. 2(a)] completely losses the attosecond structure. Nonetheless, replacing the APT with such a highly dispersive XUV pulse also produced similar photoionization oscillation. We simulated many realizations using different values of $\Delta\phi$ such as $\pi/3, 2\pi/3, \pi$ etc., and in no case did the attosecond oscillations vanished. To

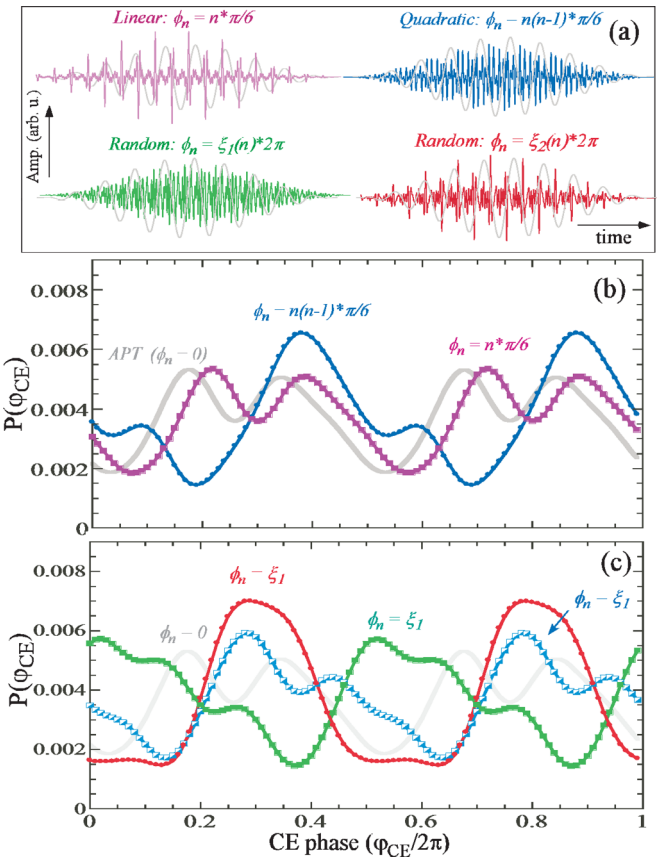

FIG. 2. (Color online) (a) XUV pulses for linear, quadratic, and random dispersions along with IR pulse. (b) The probability $P(\varphi_{\rm CE})$ versus $\varphi_{\rm CE}$ for linear and quadratic dispersion. (c) $P(\varphi_{\rm CE})$ for different random dispersions.

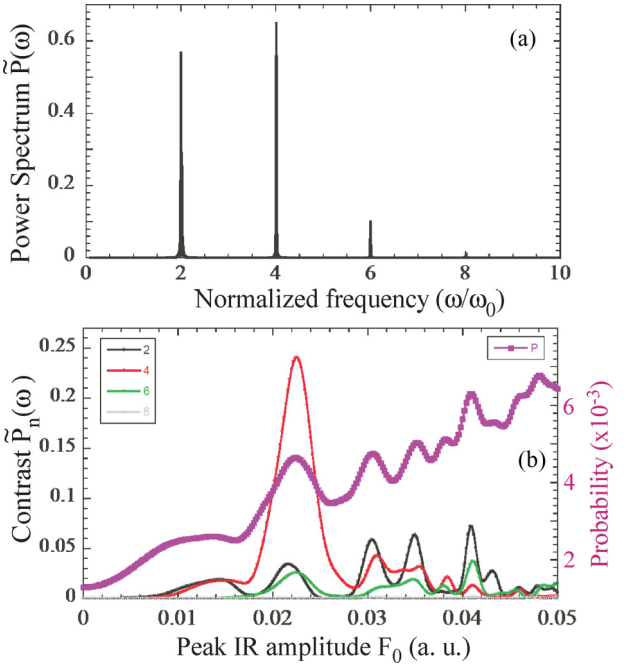

FIG. 3. (Color online) (a) The power spectral density $\tilde{P}(\omega)$ in arb. units obtained by Fourier transform of $P(\varphi_{\rm CE})$. (b) The spectral contrast in arb. units corresponding to normalized frequencies at $\omega/\omega_0 = 2$, 4, 6, and 8 versus the laser peak amplitude F_0 ($\delta\omega = 0.15\omega_0$). Note that the oscillation peak at 8 is weaker. The CE phase-averaged total ionization probability versus F_0 is also shown on the right-side axis.

show that this phenomenon is robust for arbitrary XUV dispersions, we considered a general case of random dispersion to high-order harmonic generation components. For each random realization, the phases ϕ_n are randomly chosen from a uniform probability distribution between 0 and 2π. In this case, the corresponding time structure resembles so-called broadband chaotic light as shown in Fig. 2. Surprisingly, we still obtain attosecond photoionization oscillations with remarkably similar amplitudes as compared to a phase-locked APT as shown in Fig. 2.

In order to disentangle the complex structure in the attosecond photoionization, we computed the Fourier transform $\tilde{P}(\omega)$ of $P(\varphi_{\rm CE})$. One can clearly see in Fig. 3(a) that $\tilde{P}(\omega)$ exhibits a series of sharp spikes located at even integer multiples of the IR central frequency. The peaks at $2\omega_0$, $4\omega_0$, and $6\omega_0$ were dominant and a weak one was also seen at $8\omega_0$. We quantified relative strengths of these ionization channels by defining the spectral contrast $\tilde{P}_n$,

$$\tilde{P}_n = \int_{\omega_n-\delta\omega}^{\omega_n+\delta\omega} \tilde{P}(\omega)d\omega, \tag{5}$$

where $\delta\omega$ is a frequency window centered around ω_n. Intuitively, $\tilde{P}_n$ determines the weight of the nth oscillation component (area under the peak) in total ionization. With the spectral contrast $\tilde{P}_n$ one can follow the dynamics of the individual ionization channels when, for example, the IR amplitude F_0 is varied. In Fig. 3(b) we plot the spectral contrast $\tilde{P}_n$, at one-half, one-quarter, one-sixth, and one-eighth periodicities as a function of F_0 for the case of linear dispersion. The corresponding total ionization $P(F_0)$ is also plotted on the right-side y axis. For values of $F_0 > 0.01$, we observed multiple broad resonancelike structures in $\tilde{P}_2$, $\tilde{P}_4$, and $\tilde{P}_6$. The individual oscillating components depend sensitively on the IR intensity and contribute to the total ionization P which also exhibits peaks and shoulders associated with distinct subcycle channels.

To understand the mechanism behind these oscillations we "filtered" these subcycle oscillations by analyzing the atomic response to various harmonic pairs in the XUV spectrum. In Fig. 4(a) we show three possible half-cycle oscillations in $P(\varphi_{CE})$ when three distinct pairs of neighbor harmonics are used; i.e., Eq. (3) contains only two XUV frequencies such as $11 + 13$, $13 + 15$, and $15 + 17$. These degenerate channels arise due to two-photon interferences involving one XUV photon followed by an emission or absorption of an IR photon as can be seen in Fig. 5. Similarly, when we employ a pair of harmonics separated by $4\omega_0$, e.g. ($11 + 15$, $13 + 17$, and $15 + 19$), we obtain three possible one-quarter cycle oscillations in $P(\varphi_{CE})$. These can be associated with four-photon quantum path interference involving three IR photons and one XUV photon leading to the same final state. Analogously, using harmonics separated by $6\omega_0$ and $8\omega_0$ [Fig. 4(c)] we isolate six-photon and eight-photon quantum path interference that leads to a one-sixth and a one-eighth

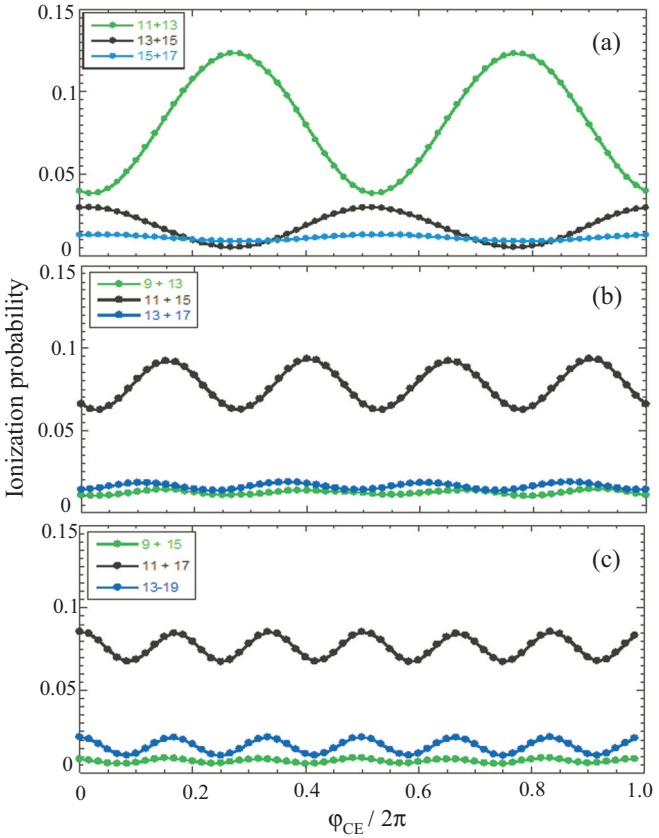

FIG. 4. (Color online) Isolation of subcycle oscillations by pairwise analysis of XUV harmonics. (a) One-half cycle oscillations at $2\omega_0$, (b) one-quarter cycle oscillations at $4\omega_0$, and (c) one-sixth cycle oscillations at $6\omega_0$. Various distinct pairs of the harmonics are labeled in the corresponding figures.

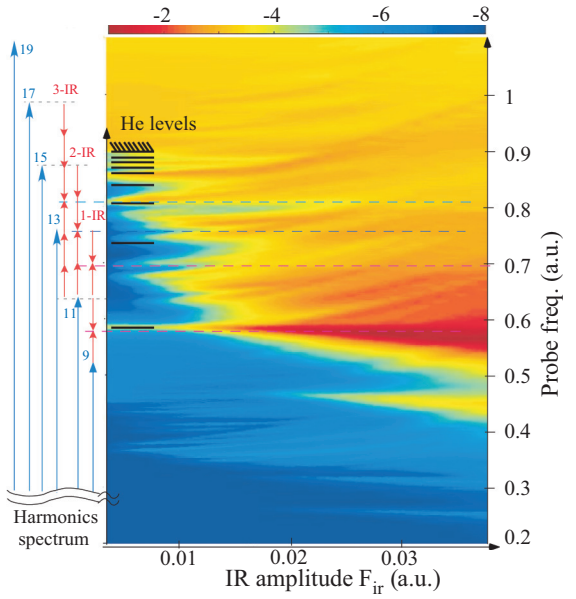

FIG. 5. (Color online) Energy levels of the undressed model shown on the right side with superimposed XUV harmonics (blue) and fundamental IR (small red arrows). The energy level structure of the dressed He atom as a function of the peak IR amplitude F_0. Different multiphoton quantum paths corresponding to two-photon (1-IR), four-photon (3-IR), and six-photon (5-IR) processes are shown by dashed lines on the level structure. The atomic levels exhibit IR-intensity-dependent shift, splitting, and broadening.

periodicity in the ionization signal, respectively. The observed good contrast in the oscillations is due to the identical number of photons involved in each interfering pathway (Fig. 5). In the general case, these subcycle oscillations are excited simultaneously, which results in complex photoionization dynamics.

Remarkably, one can improve the contrast of attosecond control of photoionization by optimizing only the phases of the harmonics without altering their spectra. Comparing for example the cases of quadratic [see Fig. 2(b)] and random phases [see Fig. 2(c)] we clearly see almost twice peak-to-peak amplitude in the net oscillation structure compared to the APT. The corresponding pulse shapes for these dispersions, shown in Fig. 2(a), appear chaotic without any attosecond bunching. In the case of such phase-randomized XUV, these features are robust and the spectral contrasts of the subcycle oscillations exhibit dependence similar to that of a function of F_0 as in Fig. 2(d). These simulations suggest that the Fourier-transform-limited pulse train may not be optimal for coherent control of electronic processes in the attosecond regime, analogous to the femtosecond coherent control [25,26]. Recently, improved time-resolution beyond the average femtosecond pulse duration was experimentally demonstrated using noisy pulses in D_2 [27].

We would like to point out that the features reported in this work are generic and robust with respect to the parameters in our model. For example, we have verified that similar subcycle oscillations were also observed when the XUV spectrum consisted of both the even and the odd harmonics (one atto pulse per cycle) and for various form of XUV dispersions. Analogous features are also expected in the photoionization or photodissociation of molecules provided the driving harmonics are scaled appropriately.

IV. SUMMARY

In conclusion, we have shown a series of subcycle oscillations in the photoionization initiated by arbitrary XUV pulses with an IR pulse at one-half, one-quarter, one-sixth, and one-eighth IR cycles. They originate from quantum path interferences between multiple IR photons and XUV harmonics which were isolated using distinct harmonic pairs. A global control of net photoionization was demonstrated by controlling the quantum superposition of subcycle ionization channels by adding various forms of linear and quadratic phase dispersion in the XUV harmonics. The interference of multiple pathways is not limited by the pulse duration of either the IR pulse or the XUV pulse. The spectral contrast for individual oscillation channels exhibit several broad resonancelike peaks when the IR intensity is varied for a fixed time-delay. Remarkably, phase-randomized XUV pulses preserve the subcycle oscillations in photoionization and their contrast could be enhanced compared to the case of a transform-limited APT. Experimental observations of such

generic subcycle oscillations should be possible with recently developed XUV pulse-shaping techniques [28,29].

This work has demonstrated the possibility for a new approach to attosecond coherent control of electronic processes in atoms and molecules by exploiting XUV dispersion [5,30–32].

ACKNOWLEDGMENTS

K.P.S. acknowledges the Department of Science and Technology, New Delhi, for support through a Ramanujan Fellowship and the Max Planck Society for a mobility grant.

[1] F. Krausz and M. Ivanov, Rev. Mod. Phys. **81**, 163 (2009).
[2] P. B. Corkum and F. Krausz, Nat. Phys. **3**, 381 (2007).
[3] Philip H. Bucksbaum, Science **317**, 766 (2007).
[4] R. Kienberger *et al.*, Science **297**, 1144 (2002).
[5] L. Gallmann, C. Cirelli, and U. Keller, Annu. Rev. Phys. Chem. **63**, 447 (2012).
[6] N. A. Papadogiannis, B. Witzel, C. Kalpouzos, and D. Charalambidis, Phys. Rev. Lett. **83**, 4289 (1999).
[7] K. P. Singh *et al.*, Phys. Rev. Lett. **104**, 023001 (2010).
[8] J. Mauritsson, P. Johnsson, E. Mansten, M. Swoboda, T. Ruchon, A. L'Huillier, and K. J. Schafer, Phys. Rev. Lett. **100**, 073003 (2008).
[9] J. Mauritsson *et al.*, Phys. Rev. Lett. **105**, 053001 (2010).
[10] P. Ranitovic, X. M. Tong, C. W. Hogle, X. Zhou, Y. Liu, N. Toshima, M. M. Murnane, and H. C. Kapteyn, Phys. Rev. Lett. **106**, 193008 (2011).
[11] P. Johnsson, J. Mauritsson, T. Remetter, A. L'Huillier, and K. J. Schafer, Phys. Rev. Lett. **99**, 233001 (2007).
[12] P. Riviere, O. Uhden, U. Saalmann, and J. M. Rost, New J. Phys. **11**, 053011 (2009).
[13] P. Ranitovic *et al.*, New J. Phys. **12**, 013008 (2010).
[14] N. Shivaram, H. Timmers, X.-M. Tong, and A. Sandhu, Phys. Rev. Lett. **108**, 193002 (2012).
[15] F. Kelkensberg *et al.*, Phys. Rev. Lett. **107**, 043002 (2011).
[16] P. Ranitovic *et al.*, Proc. Natl. Acad. Sci. U.S.A. **111**, 912 (2014).
[17] X. M. Tong, P. Ranitovic, C. L. Cocke, and N. Toshima, Phys. Rev. A **81**, 021404 (2010).
[18] X.-M. Tong and N. Toshima, Phys. Rev. A **81**, 043429 (2010).
[19] S. Chen, K. J. Schafer, and M. B. Gaarde, Opt. Lett. **37**, 2211 (2012).
[20] M. Chini *et al.*, Sci. Rep. **3**, 1105 (2013).
[21] J. Javanainen, J. H. Eberly, and Q. Su, Phys. Rev. A **38**, 3430 (1988).
[22] K. P. Singh and J. M. Rost, Phys. Rev. Lett. **98**, 160201 (2007).
[23] K. P. Singh and J. M. Rost, Phys. Rev. A **76**, 063403 (2007).
[24] M. D. Feit, J. A. Fleck, and A. Steiger, J. Comput. Phys. **47**, 412 (1982).
[25] H. Rabitz, R. de Vivie-Riedle, M. Motzkus, and K. Kompa, Science **288**, 824 (2000); I. Walmsley and H. Rabitz, Phys. Today **56**(8), 43 (2003).
[26] N. Dudovich, B. Dayan, S. M. Gallagher Faeder, and Y. Silberberg, Phys. Rev. Lett. **86**, 47 (2001).
[27] K. Meyer, C. Ott, P. Raith, A. Kaldun, Y. Jiang, A. Senftleben, M. Kurka, R. Moshammer, J. Ullrich, and T. Pfeifer, Phys. Rev. Lett. **108**, 098302 (2012).
[28] E. Gustafsson *et al.*, Opt. Lett. **32**, 1353 (2007).
[29] R. López-Martens *et al.*, Phys. Rev. Lett. **94**, 033001 (2005).
[30] A. Baltušaka *et al.*, Nature (London) **421**, 611 (2003).
[31] G. L. Yudin, A. D. Bandrauk, and P. B. Corkum, Phys. Rev. Lett. **96**, 063002 (2006).
[32] F. Lépine, M. Y. Ivanov, and Marc J. J. Vrakking, Nat. Photonics **8**, 195 (2014).